

- p 33.
 (43) E. Clar and W. Schmidt, *Tetrahedron*, **34**, 3219 (1978); **35**, 1027 (1979); **35**, 2673 (1979).
 (44) E. Clar and M. Zander, *Chem. Ber.*, **89**, 749 (1956).

- (45) R. H. Clarke and H. A. Frank, *J. Chem. Phys.*, **65**, 39 (1976).
 (46) R. Huisgen, *J. Org. Chem.*, **41**, 403 (1976).
 (47) D. Biermann and W. Schmidt, *J. Am. Chem. Soc.*, following paper in this issue.

Diels–Alder Reactivity of Polycyclic Aromatic Hydrocarbons. 2. Phenenes and Starphenes

D. Biermann and W. Schmidt*

Contribution from the Institut für Organische Chemie der Universität München, D-8000 München-2, West Germany. Received October 1, 1979

Abstract: In continuation of earlier work on the acenes and their benzologs, the second-order rate constants of 25 cata-condensed hydrocarbons of the phene and starphene type with maleic anhydride at 91.5 °C in 1,2,4-trichlorobenzene have been measured. Parallel UV measurements provided information on the structure of the Diels–Alder adducts. Two- and even three-fold addition was observed with certain hydrocarbons. The rate data could be successfully correlated with theoretical (localization energies, second-order stabilization energies) and spectroscopic (photoelectron and UV spectra) quantities. Qualitatively, the data provide support to ideas propounded long ago by Clar in the context of his sextet theory of aromaticity. The potential of these structure/reactivity relationships in checking the assumed constitution of a hydrocarbon and for detecting minute impurities is demonstrated with several examples.

Introduction

Although the stabilities of aromatic hydrocarbons have repeatedly been calculated by a variety of models (π resonance theories, localization methods), few experimental rate data were until recently available to check these theories. In the preceding paper of this series,¹ the second-order rate constants for the Diels–Alder reaction with maleic anhydride of all acenes and benzologs known to date were reported. These measurements, which were carried out in 1,2,4-trichlorobenzene at 91.5 °C, have now been extended to all other cata-condensed hydrocarbons not belonging to the above series, i.e., to the phenenes, starphenes, zigzag-annelated hydrocarbons, and helicenes. So far no experimental rate data were available for these compounds.

Unlike the acenes and their benzologs, some of these hydrocarbons react twice and even thrice with maleic anhydride, thus making the evaluation of the rate constant more difficult. There is the added complication that for some hydrocarbons the structure was uncertain; it is deduced here on the basis of the photoelectron, UV spectral, and kinetic data in conjunction with theoretical calculations described in part I. From the linearity of the $\ln E$ vs. time plot (E being the optical density at an appropriate UV absorption band of the starting hydrocarbon), minute impurities can be detected; this is particularly important for those compounds synthesized by the Elbs pyrolysis, a method known to often result in partial or complete skeletal isomerization.² Very recently, it has been recognized that this complication must also be considered for hydrocarbons prepared by photocyclodehydrogenation³ and Lewis acid catalyzed cyclodehydrogenation^{4–6} methods.

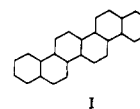
Experimental Section

Aromatic Hydrocarbons. The phenenes, starphenes, and zigzag-annelated compounds were taken from Professor Clar's collection of aromatic hydrocarbons; their synthesis is mostly described in his monograph.² The synthesis of tetrapheno(6',5':5,6)tetraphene, naphtho(2',1':1,2)tetracene, and 1,2-benzophenanthreno(9'',10'':3,4)tetracene is described in ref 7, that of tetrabenzooheptaphene in ref 8, and that of naphtho(2',3':1,2)pentacene in ref 9. The helicenes up to [14]helicene were kindly provided by Professors Martin and

Jutz, but not investigated in detail as it was quickly realized that they do not react with maleic anhydride under standard conditions.

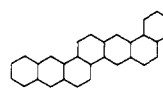
Some hydrocarbons deserve special mention in that their constitution has now been firmly established on the basis of new spectroscopic and kinetic results.

Fulminene I, not mentioned in Clar's book, was isolated in 1944

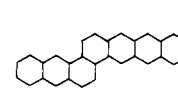


from the highest boiling fraction of coal tar; its constitution, tentatively deduced at that time on the basis of its chemical behavior, melting point, and IR spectrum,¹⁰ could now be confirmed by the photoelectron spectrum.¹¹

The sample of anthraceno(2',1':8,9)tetraphene (II), obtained in 1931 by an Elbs pyrolysis,¹² proved to contain an isomer, namely, anthraceno(2',1':1,2)tetracene (III), as shown by comparing the UV



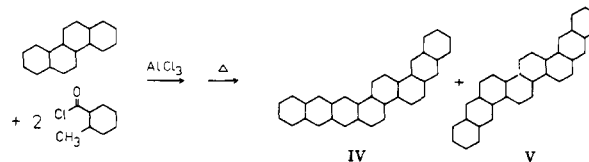
II



III

spectrum and rate behavior with those of pure III obtained by Clar¹³ in a different way. Owing to lack of material, the photoelectron spectrum of III could not yet be recorded.

Similarly, the sample believed to be 2,3-benzonaphtho(2',3':8,9)-picene (IV) was mainly tetrapheno(4',3':3,4)tetraphene (V) containing only a few percent of the expected isomer IV. They were obtained by condensing chrysene with 2 mol of *o*-toluoyl chloride and subjecting the resulting diketone to an Elbs pyrolysis:¹⁴



We shall briefly outline how this structural problem could be solved.

The specimen provided by Clar had a very diffuse UV spectrum (Figure 1) which defied simple interpretation. Repeated recrystallization from trichlorobenzene and sublimation did not change the

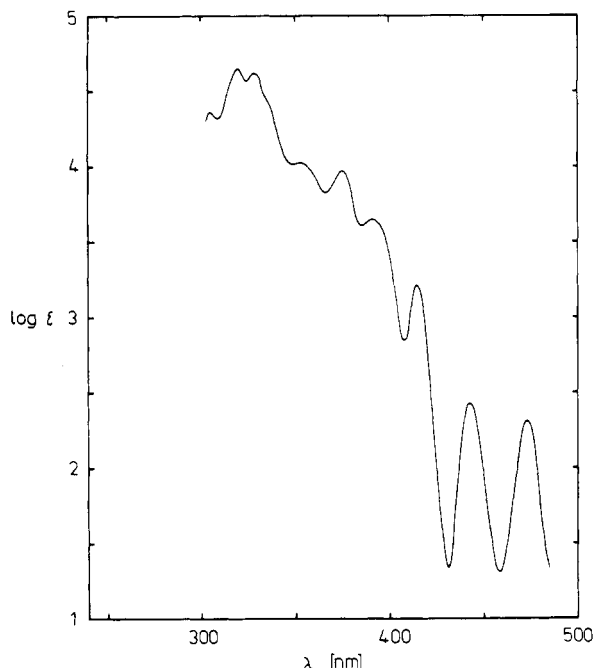


Figure 1. UV spectrum of tetrapheno(4',3':3,4)tetraphene (V) in 1,2,4-trichlorobenzene. The weak bands at 473 and 443 nm are due to a persistent impurity, namely, 2,3-benzonaphtho(2',3':8,9)picene (IV).

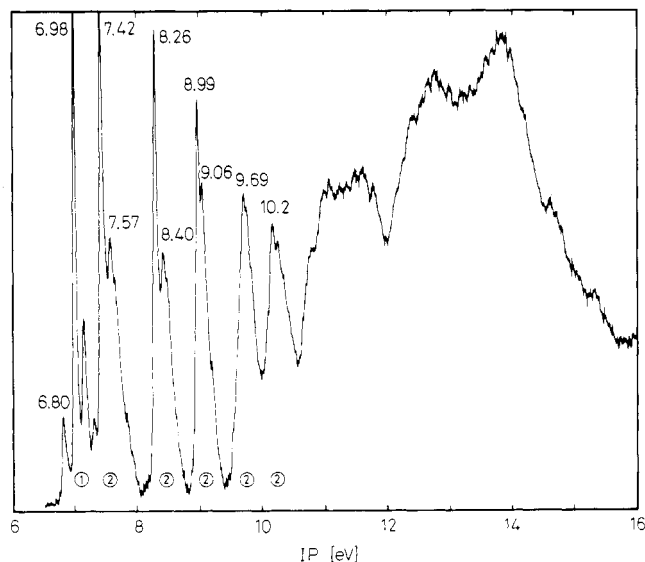


Figure 2. Photoelectron spectrum (380 °C) of tetrapheno(4',3':3,4)tetraphene (V). The weak peak at 6.80 eV is due to a persistent impurity, namely, 2,3-benzonaphtho(2',3':8,9)picene (IV). The encircled figures indicate the number of orbitals to be allotted to the various bands.

spectrum; heating the compound with copper at 410 °C to remove hydroaromatic impurities was without effect. The mass spectrum confirmed the composition $C_{34}H_{20}$; since no other molecular peaks were visible, any possible impurities must therefore be isomers.

The beautifully resolved photoelectron spectrum, shown in Figure 2, proved to be more revealing. First of all, it confirmed that we are dealing with a cata-condensed hydrocarbon (there are no extra bands at about 9 eV resulting from insular orbitals as in the pyrenes, coronenes, perylenes, and peropyrenes) and that it contains about 33 carbon atoms (there are 11 IPs out to 10.5 eV). However, the observed first IP of 6.98 eV definitively excludes IV since, according to the Hückel calculation, the naphthotetracene chromophore present in IV should give rise to a first IP of 6.80 eV; for comparison, naphtho(2',1':1,2)tetracene has $IP_1 = 6.83$ eV.

Providing that the two toluoyl chlorides attacked different naphthalene sites of the chrysene molecule and that the Elbs pyrolysis did

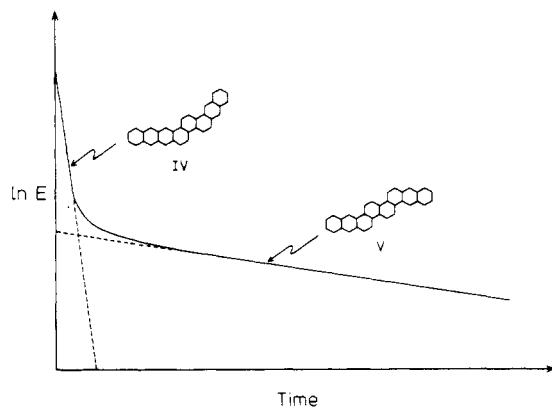
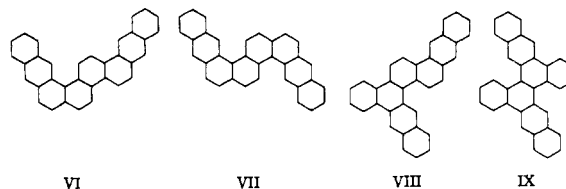


Figure 3. Spectrophotometric determination of the rate constant k_2 of the Diels–Alder reaction of tetrapheno(4',3':3,4)tetraphene (V) containing 2,3-benzonaphtho(2',3':8,9)picene (IV) as a persistent impurity with excess maleic anhydride (pseudo-first-order rate behavior).

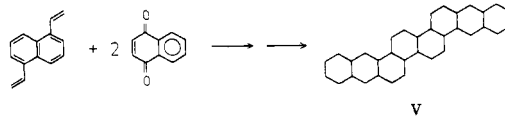
not isomerize the chrysene unit, we may discuss, besides V, the alternatives VI–IX. VI–IX must be rejected because they encompass



nonplanar 3,4-benzophenanthrene units which would make their photoelectron spectra diffuse. In addition, IX is known;⁷ its photoelectron spectrum bears no resemblance to that of Figure 2. Finally, the IP_1 to IP_{11} values calculated by Hückel theory, while not definitively excluding VI and VII, nevertheless favor V.

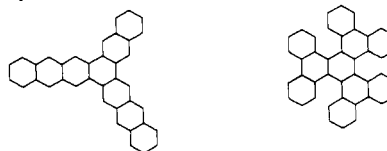
The rate constant k_2 measured for Clar's hydrocarbon agrees satisfactorily with that calculated by second-order perturbation theory (cf. part 1) for V–VIII. After completion of the reaction, the UV spectrum of the Diels–Alder adduct showed the characteristic bands of the chrysene chromophore at 380, 361, and 347 nm, thus confirming that the central chrysene unit remained intact in the course of the Elbs pyrolysis.

The $\ln E$ vs. time plot (Figure 3) showed at the same time that the sample contained an impurity whose k_2 value (32 times larger than that of the main component) is consistent with structure IV originally proposed by Clar. This impurity also shows up in the photoelectron spectrum as a weak peak at 6.80 eV, a value which perfectly fits the naphthotetracene range and thus supports structure IV. Based on these findings we can now also understand the complicated UV spectrum. The peaks at 473 and 443 nm are the first two vibrational components of the p band of the naphthotetracene chromophore present in IV (naphthotetracene in the same solvent has peaks at 476 and 446 nm). By reacting the hydrocarbon mixture with maleic anhydride for an appropriate period of time so as to remove IV, the UV spectrum simplified considerably and proved to be identical with that of tetrapheno(4',3':3,4)tetraphene (V) synthesized in an unambiguous manner by Zander¹⁵ starting from 1,5-divinylnaphthalene:



The identity of Clar's and Zander's hydrocarbons is further demonstrated by a comparison of their IR spectra.

By similar experiments a persistent impurity of unknown constitution was detected in tetrabenzoheptaphene, and the structures of two long-known hydrocarbons, namely, [3.3.2]starphene¹⁶ and hexabenzotriphenylene,¹⁷ turned out to be incorrect; owing to lack of



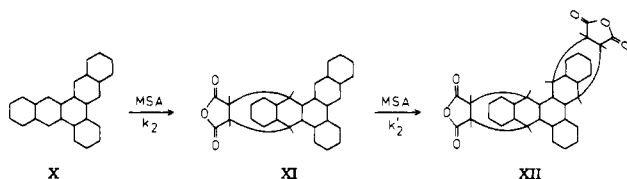
material and diffuseness of the spectra, their true constitution could not yet be deduced.

All other hydrocarbons relevant to the present work and to part I have been assigned correct structures in the literature, and they may be considered as "pure" on the basis of the photoelectron, UV, MS, and kinetic data.

Evaluation of the Rate Constants. The kinetic and spectroscopic measurements were carried out as in part I. For pure hydrocarbons, the second-order rate constant k_2 is independent of which UV absorption band is monitored. In order to minimize overlap with the absorption bands of maleic anhydride and the Diels–Alder adduct, usually the longest wavelength band was chosen.

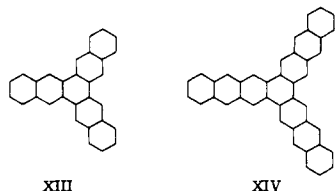
For hydrocarbons containing persistent impurities, e.g., the pair IV and V, the rate constant of each component is most conveniently evaluated by choosing an absorption band at which this component absorbs selectively. In the case of IV, the bands at 443 and 473 nm (cf. Figure 1) fulfill this condition. For V the bands at 414.5 or 375 nm may be chosen. However, as IV absorbs also at these wavelengths, we obtain a $\ln E$ vs. time diagram of the form shown in Figure 3. The rate constant deduced from the slope of the initial fast decay of $\ln E$ (after base-line correction) agrees, within experimental error, with that measured for IV at 443 or 473 nm. The subsequent slow decay then yields the rate constant of V. It should be emphasized that the evaluation of the k_2 values along these lines requires no prior knowledge of the molar ratio of the two components or their extinction coefficients.

In contrast to the hydrocarbons considered in part I, the phenes and starphenes are able to add two or even three molecules of maleic anhydride (MSA) with comparable ease so that the rate constant k_2 cannot be directly determined. Consider 6,7-benzopentaphene as an example. If the Diels–Alder reaction is monitored using the longest wavelength band at 391 nm, the optical density goes first through a maximum because of the buildup of the intermediate XI which absorbs also at 391 nm, and then decays exponentially (the final adduct XII does not absorb at this wavelength as it contains only benzene and



naphthalene chromophores). The kinetic equations for this consecutive reaction were solved on an analog computer by systematically varying the two rate constants, k_2 and k_2' , and the extinction coefficient of XI until the experimental E vs. time curve was reproduced (cf. Figure 4). The rate constant of interest, k_2 , can also be extracted, with greater accuracy, from the exponential part of the E vs. time curve (after about 15 h the decay is exponential).

This procedure could also be applied to naphtho(2',3':6,7)pentaphene (XIII), which consecutively adds three molecules of maleic



anhydride, but it failed for anthraceno(2',3':7,8)heptaphene (XIV) because of lack of a suitable absorption band.

Results and Discussion

Table I contains the following data: firstly, the structures of the primary Diels–Alder adducts, as deduced from the UV spectra of the reaction mixtures taken at regular intervals; secondly, the second-order rate constants k_2 measured at 91.5 °C in 1,2,4-trichlorobenzene; thirdly, the two IPs that relate to the first sharp and first diffuse photoelectron bands, i.e., to the occupied orbitals of highest angular quantum number λ (these IPs are usually the first and second ones and, for simplicity, have therefore been termed IP₁ and IP₂); fourthly, the energies of the 0–0 components of the three main UV transi-

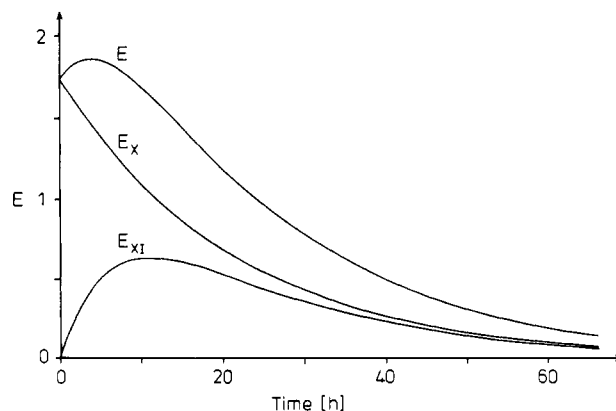


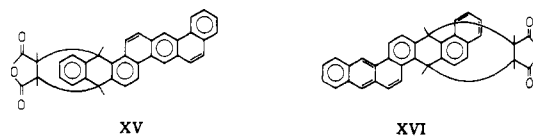
Figure 4. Computer simulation of the twofold Diels–Alder reaction of 6,7-benzopentaphene (X) with maleic anhydride. E_X and E_{XI} are the optical densities of X and XI, respectively, at 391 nm; E is the sum of both (see text).

tions, as estimated from the solution spectra according to the procedure described in part I.

Table II gives the three theoretical quantities which in part I proved useful in correlating and interpreting the rate and regioselectivity data, namely, the para-localization energies P , the structure count ratios SC_P/SC_R , and the total second-order stabilization energies $\Sigma E^{(2)}$; these were evaluated as before¹ and refer to the meso positions predicted to be the most reactive ones in a given hydrocarbon. The free valences and Dewar numbers are also available but will not be considered further as they closely mimic the para-localization energies. Resonance energies calculated by the Hess–Schaad scheme were kindly provided by Professors Hess and Schaad; the results will be published separately.

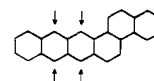
Regioselectivity. It is most encouraging that all theoretical indexes lead, without exception, to identical results regarding the reactive meso positions. Where the structures of the adducts have been unambiguously determined, these predictions are in full agreement with experiment. The zigzag-annulated hydrocarbons and the helicenes are predicted to react at the terminal benzo rings; however, this cannot be tested as they do not react with maleic anhydride under standard conditions.

Interestingly, Clar's simplified treatment^{2,18} also leads to correct results. For example, anthraceno(2',1':8,9)tetraphene with two anthracene chromophores is predicted (and found) to give adduct XV with four sextets and not XVI with only



three. This result can be restated by saying that among two acene units of the same length the less annulated one is preferentially attacked. In XV this is a tetraphene-type branch which is much more reactive¹ than the 1,2:5,6-dibenzanthracene branch in XVI.

In hydrocarbons with two acene units of different length, the longer one is found to be more reactive, in accord with Clar's postulates. If this is an even-numbered acene, such as in naphtho(2',1':1,2)tetracene, then there are two reactive meso



sites (indicated above by arrows) between which Clar's theory does not distinguish as the resulting adducts would both have three sextets. In such situations the rule¹ is valid that the di-

Table I. Second-Order Rate Constants k_2 ($\text{L M}^{-1} \text{s}^{-1}$) and Their Logarithms, IP_1 and IP_2 (eV), and Energies of the α -, p-, and β -Absorption Bands in the Gas Phase (eV)^a

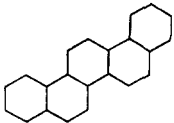
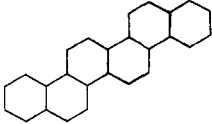
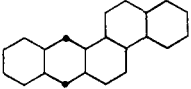
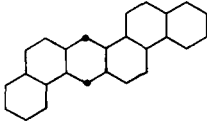
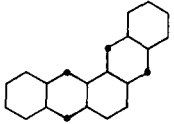
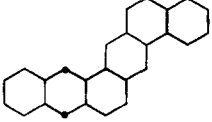
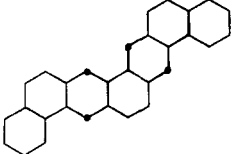
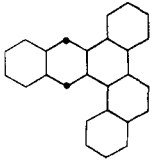
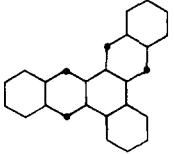
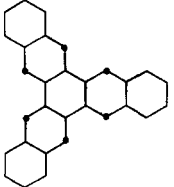
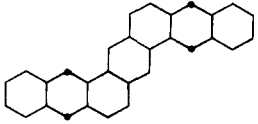
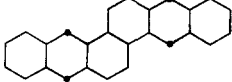
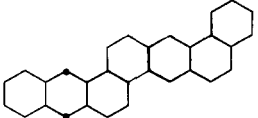
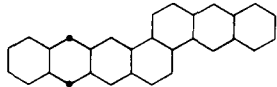
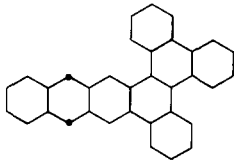
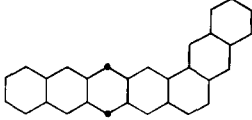
hydrocarbon		$10^6 k_2$	$6 + \log k_2$	IP_1	IP_2	E_α	E_p	E_β
picene				7.50	7.74	3.29	3.80	4.32
fulminene				7.36	7.70	3.22	3.66	4.23
3,4-benzotetraphene		383	2.58	7.20	8.24		3.27	4.42
3,4:8,9-dibenzotetraphene		28	1.45	7.19	7.74	3.14	3.39	4.11
pentaphene		66	1.82	7.27	7.39	2.96	3.55	3.95
3,4-benzopentaphene		55	1.74	7.20	7.44	2.97	3.42	3.91
3,4:9,10-dibenzopentaphene		8	0.91	7.11	7.44	2.97	3.43	3.88
1,2:5,6-dibenzotetraphene		142	2.15	7.15	7.73	3.09	3.27	3.99
6,7-benzopentaphene		60	1.78	7.36	7.57	3.18	3.63	4.06
naphtho(2',3':6,7)pentaphene		58	1.77	7.35	7.35	3.07	3.62	3.95
naphtho(2',3':3,4)pentaphene		99	2.00	7.04	7.48	2.89	3.28	3.76
anthraceno(2',1':1,2)anthracene		1060	3.03	6.98	7.91		3.02	4.10
anthraceno(2',1':8,9)tetraphene		475	2.68	6.97	7.75		3.10	3.88

Table I (Continued)

hydrocarbon		$10^6 k_2$	$6 + \log k_2$	IP ₁	IP ₂	E_α	E_p	E_β
tetrapheno(9',8':8,9)tetraphene		66	1.82	6.96	7.58	2.96	3.18	3.82
tetrapheno(6',5':5,6)tetraphene		160	2.20	6.83	7.74		2.97	3.84
2,3-benzopicene		277	2.44	7.17	7.61	3.04	3.34	3.94
2,3:8,9-dibenzopicene		421	2.62	7.17	7.34	2.94	3.37	3.78
tetrapheno(4',3':3,4)tetraphene		844	2.93	6.98	7.57	2.96	3.09	3.88
hexaphene		6670	3.82	6.92	7.39	2.70	2.94	3.61
heptaphene		9320	3.97	6.89	6.89	2.43	2.97	3.27
7,8-benzoheptaphene		7930	3.90	6.90	6.90	2.56	2.93	3.30
1,2:3,4:11,12:13,14-tetrabenzoheptaphene		393	2.59	6.88	6.88	2.56	3.06	3.31
naphtho(2',1':1,2)tetracene		25 500	4.41	6.83	7.91		2.72	3.99
2,3-benzonaphtho(2',3':8,9)picene		26 600	4.43	6.80	7.80 ^b		2.75	

Table I (Continued)

hydrocarbon		$10^6 k_2$	$6 + \log k_2$	IP ₁	IP ₂	E_α	E_p	E_β
anthraceno(2',1':1,2)tetracene		24 800	4.39	6.65 ^b	8.00 ^b		2.65	
1,2-benzophenanthreno(9'',10'':3,4)-tetracene		8 490	3.93	6.73	7.85		2.73	3.86
naphtho(2',3':1,2)pentacene		234 000	5.37	6.59	7.33		2.39	3.29

^a The dots in the structural formulas indicate the most reactive meso positions. The rate constants are not corrected for statistical factor.

^b IPs of anthracenotetracene and benzonaphthopentacene (IP₂ only) extrapolated.

Table II. Para-Localization Energies P , Structure Count Ratios SC_P/SC_R , and Total Stabilization Energies $\Sigma E^{(2)}$ for the Most Reactive Meso Positions

hydrocarbon	$P[\beta]$	SC_P/SC_R	$\Sigma E^{(2)}[\beta^2]$
picene	-3.7510	8/13	-0.1399
fulminene	-3.7488	13/21	-0.1403
3,4-benzotetraphene	-3.3907	10/11	-0.1484
3,4,8,9-dibenzotetraphene	-3.4894	15/19	-0.1451
pentaphene	-3.4490	8/10	-0.1451
3,4-benzopentaphene	-3.4378	14/17	-0.1463
3,4,9,10-dibenzopentaphene	-3.5320	21/29	-0.1433
1,2,5,6-dibenzotetraphene	-3.4702	16/20	-0.1458
6,7-benzopentaphene	-3.5130	14/19	-0.1436
naphtho(2',3':6,7)pentaphene	-3.5276	20/28	-0.1428
naphtho(2',3':3,4)pentaphene	-3.4337	20/24	-0.1466
anthraceno(2',1':1,2)anthracene	-3.3827	14/15	-0.1491
anthraceno(2',1':8,9)tetraphene	-3.3862	24/26	-0.1494
tetrapheno(9',8':8,9)tetraphene	-3.4853	36/45	-0.1455
tetrapheno(6',5':5,6)tetraphene	-3.4528	40/48	-0.1469
2,3-benzopicene	-3.4001	16/18	-0.1485
2,3,8,9-dibenzopicene	-3.4036	22/25	-0.1484
tetrapheno(4',3':3,4)tetraphene	-3.3962	36/40	-0.1489
hexaphene	-3.2893	14/13	-0.1525
heptaphene	-3.2945	18/17	-0.1525
7,8-benzoheptaphene	-3.3061	34/33	-0.1524
1,2,3,4,11,12,13,14-tetrabenzoheptaphene	-3.4374	153/185	-0.1468
naphtho(2',1':1,2)tetracene	-3.2691	16/14	-0.1539
2,3-benzonaphtho(2',3':8,9)picene	-3.2740	36/32	-0.1540
anthraceno(2',1':1,2)tetracene	-3.2666	22/19	-0.1545
1,2-benzophenanthreno(9'',10'':3,4)tetracene	-3.2870	48/44	-0.1539
naphtho(2',3':1,2)pentacene	-3.2232	21/16	-0.1563

enophile attacks the less strongly annelated site of the acene.

The congruence (and success) of these six indexes in predicting the positional selectivity is particularly surprising as they start from different assumptions. The para-localization concept and the Clar and Hess-Schaad theories presume a late transition state and predict the adduct with the largest π -electron energy (or largest sextet number) to be formed, whereas second-order perturbation theory and the free valence concept argue on the basis of the different reactivities of the various meso positions in the starting hydrocarbon (early transition state). In other words, there must be some common algebra behind these concepts, and the thermodynamically most stable adduct seems to be favored also on kinetic grounds.

This monotonic relationship between activation energy and reaction enthalpy (Hammond's postulate) need not necessarily hold also in the nonalternant series, e.g., the fluoranthenes, so that one might be able to define the nature of the transition state more clearly.

However, using the structure-count correlation reported in the next section (cf. Figure 6), a rough experimental estimate for the position of the transition state along the reaction coordinate can be provided. Herndon²⁰ has shown that the change in π -resonance energy between adduct and starting hydrocarbon is given by

$$\Delta RE \text{ (kcal/mol)} = 27.33 \ln (SC_P/SC_R) \quad (1)$$

These ΔRE values closely mimic the results of highly elaborate SCF calculations and should thus correlate well with the reaction enthalpies ΔH . Since the activation entropies may be assumed to be the same for all reactions and since all reactions were performed at the same temperature, an Arrhenius-type relationship between activation enthalpies and $\log k_2$ values should hold:

$$\Delta H^\ddagger = \text{const} - 2.303RT \log k_2 \quad (2)$$

The least-squares regression of the $\log k_2$ values for all hydrocarbons of parts 1 and 2 on the $\ln (SC_P/SC_R)$ values yields

$$6 + \log k_2 = 3.323 + 7.006 \ln (SC_P/SC_R) \quad (3)$$

Substituting $\ln (SC_P/SC_R)$ from eq 1 and $\log k_2$ from eq 2 into eq 3 gives

$$\Delta H^\ddagger = \text{const} + 6.165RT - 0.590RT\Delta RE \quad (4)$$

The slope of the ΔH^\ddagger vs. ΔRE regression is -0.43 , suggesting that 43% of the reaction enthalpy is reflected in the transition state. Thus, the generally accepted¹⁹ "early" transition state of Diels-Alder reactions seems to accord with our data. However, as the above estimate depends critically on the proportionality factor in eq 1, independent evidence from measurements of the reaction enthalpies should be sought. Work along these lines is in progress.

The precise stereochemistry (endo/exo) of the adducts cannot be deduced from their UV spectra, requiring a more sensitive technique like ¹³C NMR. Such experiments remain to be done.

Rate Constants. Theoretical Correlations. Linear regressions of the $6 + \log k_2$ data (corrected for multiple reaction sites) for all compounds of parts 1 and 2 on the various theoretical indexes yield the following standard deviations:

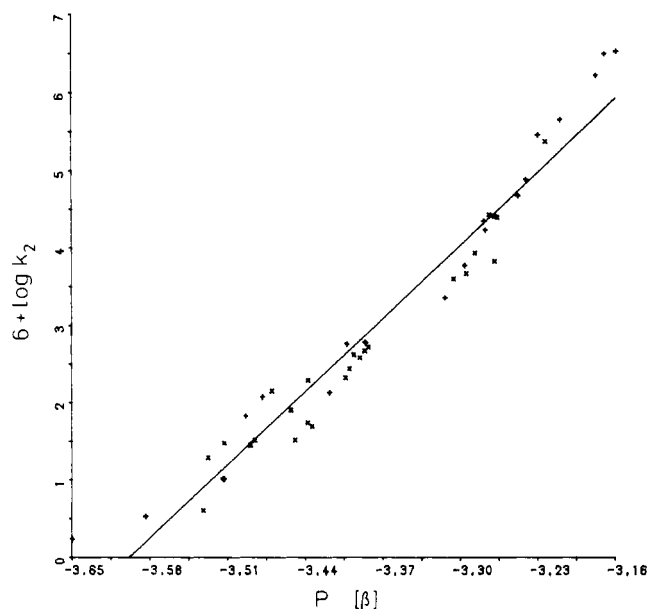


Figure 5. Plot of rate data (corrected for statistical factor) on the para-localization energies P , 46 data points (+, acenes and benzologs; x, phenes and starphenes). Least-squares regression: $6 + \log k_2 = 48.53 + 13.49P$.

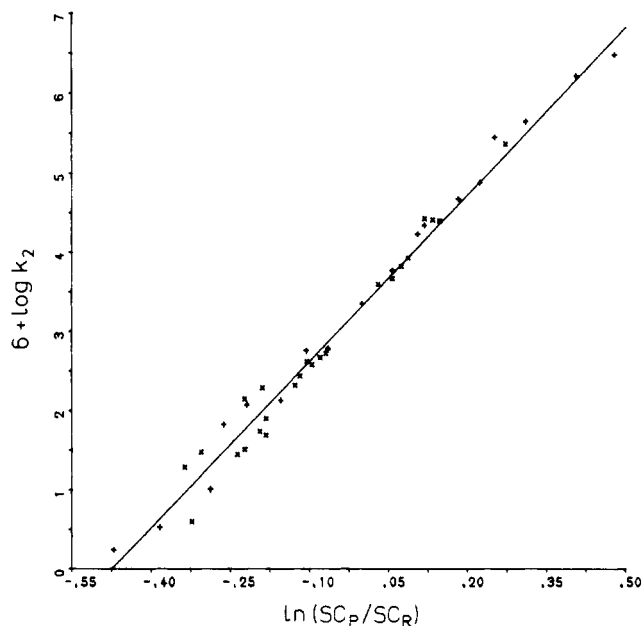


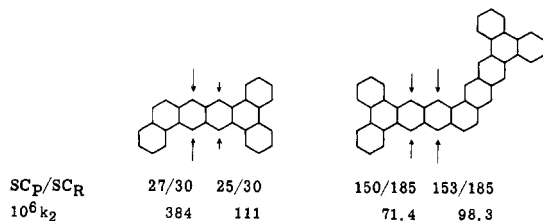
Figure 6. Plot of rate data (corrected for statistical factor) on logarithms of structure count ratios SC_P/SC_R , 46 data points. Least-squares regression: $6 + \log k_2 = 3.323 + 7.006 \ln(SC_P/SC_R)$.

para-localization energies P	0.361
structure count indexes $\ln(SC_P/SC_R)$	0.227
Hess-Schaad resonance energy differences $RE_P - RE_R$	0.218
Dewar numbers $N_r + N_s$	0.250
second-order stabilization energies $\Sigma E^{(2)}$	0.274
free valence indexes ΣF_μ	0.325

According to an F test (44 degrees of freedom, 95% security), all theories except the free valence concept are superior to the para-localization method. Interestingly, this applies also to the Dewar numbers, which are nothing but a very crude approximation to the para-localization energies. The success of the structure count method—the simplest of the six theories examined—is also noteworthy.

The regressions with the para-localization energies, the structure count indexes, and the second-order stabilization energies are shown in Figures 5–7.

Closer examination of the structure count and Hess-Schaad plots shows that some hydrocarbons such as tribenzotetracene or tetrabenzoheptaphene react faster than predicted by the theoretical indexes. This discrepancy is presumably due to the fact that regioselectivity is not strict; i.e., the assumption of integer statistical factors (one for tribenzotetracene, two for tetrabenzoheptaphene) is not justified. Using the structure count correlation, eq 3, the rate constants for the meso positions marked below by arrows are predicted to be as follows:



The statistical factors calculated from these rate constants are 1.29 for tribenzotetracene and 3.45 for tetrabenzoheptaphene. This complication must be considered for all hydrocarbons comprising long acene chromophores; the quality of the plot shown in Figure 6 is considerably improved if fractional statistical factors are used to correct the measured rate constants.

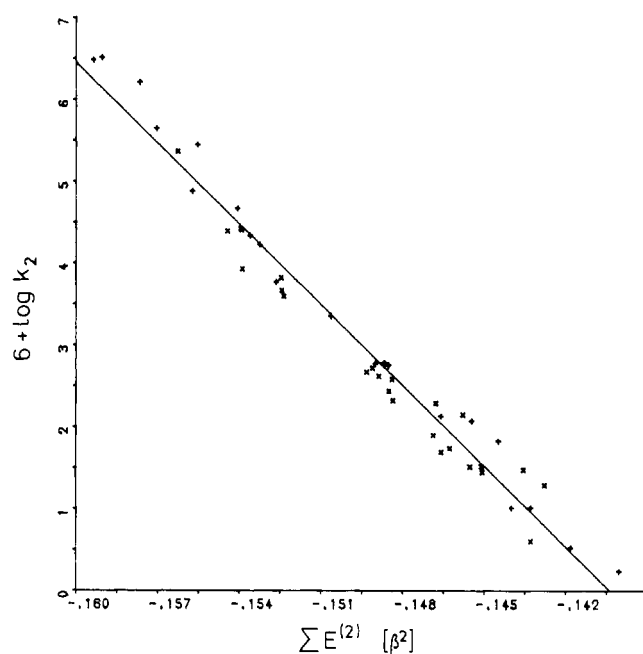


Figure 7. Plot of rate data (corrected for statistical factor) on the total second-order stabilization energies $\Sigma E^{(2)}$, 46 data points. Least-squares regression: $6 + \log k_2 = -46.08 - 328.33 \Sigma E^{(2)}$.

Rate Constants. Empirical Correlations. In part 1 it was shown that $\Delta IP = IP_2 - IP_1$ or, better, $0.347IP_2 - 0.653IP_1$ parallel the second-order stabilization energies $\Sigma E^{(2)}$ so that the rate constants could be successfully correlated with IPs taken from the photoelectron spectra. It was of interest, therefore, to see whether this holds also for the phenes and starphenes.

A plot of $0.347IP_2 - 0.653IP_1$ against $\Sigma E^{(2)}$ shows good linearity. There are some notable exceptions, however. Compounds comprising two acene branches of the same length, such as heptaphene, deviate significantly from the regression line. As a result of this, the fit of the $\log k_2$ values on the IPs is definitely worse than that for the acenes and their benzologs alone, even if a statistical correction is applied.

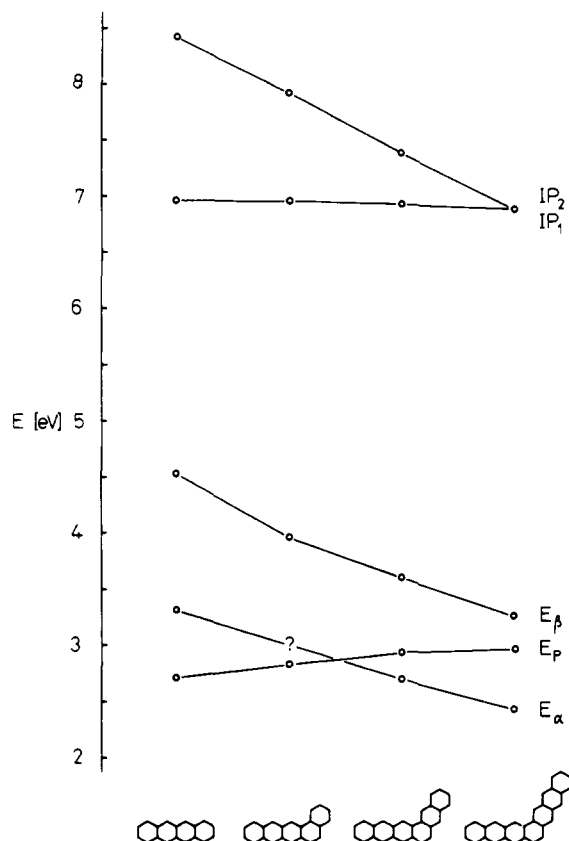


Figure 8. Correlation diagram, showing the effect of angular annelation on the UV band energies and first two IPs of tetracene.

Since there is a direct physical relation between the UV and the photoelectron data,¹¹ precisely the same results are obtained if the $\log k_2$ values are correlated with the p- and β -band energies.

Although it is evident that the photoelectron data offer no general solution to the reactivity problem, some useful insights into the relation between structure and reactivity are possible. This is due to the fact that the two crucial IPs can be predicted with sufficient accuracy by either using simple additivity rules¹¹ for linear vs. angular annelation or by considering the basic segments in the hydrocarbons.²¹ For example, the first IP in the following series of compounds is roughly constant at

$10^6 k_2$	47.100	16.950	6.670	4.680
IP ₁	6.97	6.98	6.92	6.89
IP ₂	8.41	7.92	7.39	6.89
ΔIP	1.44	0.96	0.47	0.0

6.9 eV, i.e., the IP₁ value of the longest linear chromophore which is of the tetracene type in all four hydrocarbons. The second IP can be related to the second branch which is of the benzene, naphthalene, anthracene, and tetracene type, respectively. That is, the second IP decreases steadily across the series until, in the last member, it coincides with the first IP. As a result of the decreasing ΔIP values, the ratio constant diminishes by a factor of 10.

If photoelectron spectra are not available, precisely the same conclusions can be drawn from the UV spectra. In Figure 8 are correlated, for the above series, the energies of the three main UV bands together with the first two IPs to which the UV bands are related.²² The p-band energy changes very little across the series as does the first IP. However, owing to the increasing molecular size, $IP = \frac{1}{2}(IP_1 + IP_2)$ decreases so that

the α - and β -band energies are lowered. This causes the α and p bands to cross between the second and third members of the series. Thus, whereas the highly reactive tetracene has the band sequence p before α , the much less reactive heptaphene has α before p. Equivalently, we may take the difference in the β - and p-band energies as an indicator of reactivity.

An equally instructive annelation series starts with anthracene. The trends in the first two IPs can be analyzed as

$10^6 k_2$	2270	136	33	30	19
IP ₁	7.41	7.41	7.27	7.36	7.35
IP ₂	8.54	8.04	7.39	7.57	7.35
ΔIP	1.13	0.63	0.12	0.21	0.0

above. The drastic reduction of ΔIP , in going from anthracene to pentaphene with two branches of the same length, is reflected in a decrease of k_2 by almost two powers of ten. Annelation in the third direction lowers IP₃ but does not affect IP₁ and IP₂ (and therefore ΔIP) very much so that k_2 now remains roughly constant.

These examples emphasize once more^{1,11} that hydrocarbons with large ΔIP (that is, p before α in the UV spectrum) exhibit high Diels-Alder reactivity, whereas those with small or zero ΔIP (that is, α before p) react only with difficulties or are inert. The condition $\Delta IP = 0$ is most likely met for symmetry reasons. Indeed, photoelectron spectroscopy shows that IP₁ and IP₂ coincide in all hydrocarbons with trigonal (triphenylene, naphtho(2',3':6,7)pentaphene, etc.) or hexagonal symmetry (benzene). The extreme chemical stability of highly symmetrical hydrocarbons, which was noted by many authors (e.g., ref 2 and 18), is certainly related to this fact. Very small ΔIP values are also found among compounds exhibiting a high degree of angular, zigzag, or helical annelation. The orbital energy spectrum of these hydrocarbons is strikingly similar to that of the pertinent $(4n + 2)$ annulene, with all occupied orbitals except the lowest one appearing in near-degenerate pairs, so that it is appropriate to call them "annulenoid".¹ Small ΔIP values also typify²³ the "fully benzenoid" hydrocarbons, a class of compounds distinguished by extreme stability.¹⁸

As far as phosphorescence data are available for the present compounds,²⁴ they confirm the rule¹ that hydrocarbons with high triplet half-lifetime $\tau_{1/2}$, such as picene (1.7 s), [5]helicene (1.7 s), and [6]helicene (1.5 s), show no noticeable Diels-Alder reactivity, and vice versa. For those compounds for which both $\tau_{1/2}$ and k_2 are available, their product appears to be roughly constant: pentaphene (0.5 s), naphtho(2',3':6,7)pentaphene (0.5 s), and tetrapheno(6',5':5,6)tetraphene (0.1 s) yield $10^6 k_2 \tau_{1/2}$ values of 17, 10, and 8, respectively, after correcting for a statistical factor.

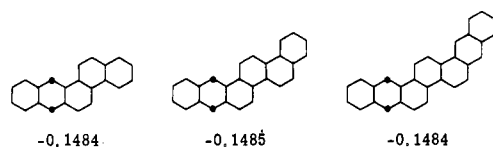
Further experimental and theoretical work is needed to better understand the basis of this relationship. It will be interesting to see whether the rate data correlate also with other properties of the lowest triplet state, for example, with the zero-field splitting parameter $|D|$ which is a measure of the dipole-dipole interaction of the triplet electrons. Since the spin density is highest at the reactive meso positions (see discussion of the frontier orbital model in part 1), some correlation with reactivity might be anticipated.

Rate Constants. Qualitative Trends. Needless to say, the trends discussed in the preceding section are correctly reproduced by Clar's theory. In going from tetracene to 1,2-benzotetracene, a new sextet is created, resulting in a decrease of k_2 . Increasing the length of the second branch does not generate a new sextet so that k_2 should remain approximately constant, in accord with experiment. Similar comments apply to the annelation series beginning with anthracene.

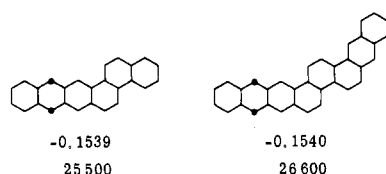
Even finer details are predicted, e.g., the decrease of k_2 in going from heptaphene with two sextets to 7,8-benzoheptaphene with three, or in going from pentaphene (two sextets) to 6,7-benzopentaphene and naphtho(2',3':6,7)pentaphene (three sextets). The great chemical stability of the helicenes and zigzag annelated compounds and the very low reactivity of hydrocarbons such as 3,4,9,10-dibenzopentaphene (four sextets among seven rings) are satisfactorily explained.

The success of Clar's treatment prompted us to examine whether the measured k_2 values allow partial structures to be recognized within larger hydrocarbons. In many homologous series, this proved to be the case.

For example, second-order perturbation theory yields the same $\Sigma E^{(2)}$ values for the following three hydrocarbons:



This is largely borne out by the measured $10^6 k_2$ values of 383, 277, and 211, respectively (statistical correction applied for the third hydrocarbon). In other words, the k_2 value of the latter two hydrocarbons is largely characteristic of the 3,4-benzotetraphene chromophore and not of the molecules as a whole. This argument explains also the similarity of the $\Sigma E^{(2)}$ and $10^6 k_2$ values of the following pair:



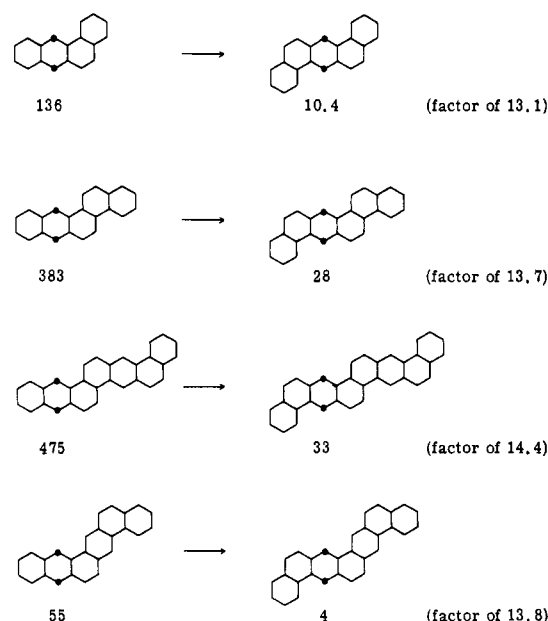
The structure count method leads to precisely the same results.

Even more surprising regularities are summarized in Chart I. In going from tetraphene to 1,2:5,6-dibenzanthracene, i.e., by adding an angular benzo rest in anti position, the $10^6 k_2$ value reduces by a factor of 13.1. Within experimental error, this factor holds also for the other three pairs.

It is obvious that these observations allow us to predict the rate behavior of a host of yet unknown compounds with sufficient accuracy or, conversely, to deduce the (unknown) constitution of a hydrocarbon from its mass spectrum and rate constant, the latter requiring less than 0.1 mg of substance and usually only a few hours time.

The fact that the rate behavior can be described in such simple terms attests that the Diels-Alder reaction of aromatic hydrocarbons with maleic anhydride has negligible steric demand and that the activation entropies are either constant or parallel the k_2 values. Activation parameters measured at five temperatures between 70.5 and 112.5 °C are now available for some selected compounds; the ΔS^\ddagger values seem to be fairly constant, lying between -30.0 ± 0.5 eu for anthracene and -33.5 ± 0.7 eu for anthraceno(2',3':1,2)coronene. In other words, aromatic hydrocarbons are ideal substrates for studying the interplay between (electronic) structure and reactivity.

Chart I



Acknowledgments. We have pleasure in acknowledging the constant help of Professor E. Clar, who kindly placed his collection of aromatic hydrocarbons at our disposal. We also thank Mr. K. D. Baumgart for synthesizing 1,5-divinylnaphthalene and tetrapheno(4',3':3,4)tetraphene.

References and Notes

- (1) D. Biermann and W. Schmidt, *J. Am. Chem. Soc.*, preceding paper in this issue. Both papers were presented at the International Symposium on Aromaticity, Dubrovnik, Yugoslavia, Sept 3-5, 1979.
- (2) E. Clar, "Polycyclic Hydrocarbons", Vol. I, Academic Press, New York, 1964.
- (3) A. H. A. Tinnemans and W. H. Laarhoven, *J. Am. Chem. Soc.*, **96**, 4611, 4617 (1974).
- (4) G. P. Blümer, K. D. Gundermann, and M. Zander, *Chem. Ber.*, **109**, 1991 (1976).
- (5) D. Lavit-Lamy and N. P. Buu-Hoi, *Chem. Commun.*, 92 (1966).
- (6) F. A. Vingiello, J. Yanez, and J. A. Campbell, *J. Org. Chem.*, **36**, 2053 (1971).
- (7) E. Clar, J. F. Guye-Vuillème, and J. F. Stephen, *Tetrahedron*, **20**, 2107 (1964).
- (8) C. C. Mackay, Ph.D. Thesis, University of Glasgow, 1971.
- (9) E. Clar and B. A. McAndrew, *Tetrahedron*, **28**, 1237 (1972).
- (10) E. Clar and K. F. Lang, unpublished experiments, 1944. Cf. also K. F. Lang, *Angew. Chem.*, **63**, 345 (1951); K. F. Lang, H. Buffleb, and J. Kalowy, *Chem. Ber.*, **97**, 494 (1964).
- (11) W. Schmidt, *J. Chem. Phys.*, **66**, 828 (1977).
- (12) J. W. Cook, *J. Chem. Soc.*, 499 (1931).
- (13) E. Clar and W. Kelly, *J. Am. Chem. Soc.*, **76**, 3502 (1954).
- (14) E. Clar and J. F. Guye-Vuillème, unpublished experiments, 1962.
- (15) M. Zander and W. H. Franke, *Chem. Ber.*, **107**, 727 (1974).
- (16) E. Clar and A. Mullen, *Tetrahedron*, **24**, 6719 (1968).
- (17) J. G. Carry and I. T. Millar, *J. Chem. Soc.*, 3144 (1959).
- (18) E. Clar, "The Aromatic Sextet", Wiley, New York, 1972.
- (19) R. Huisgen, *J. Org. Chem.*, **41**, 403 (1976).
- (20) R. Swinborne-Sheldrake, W. C. Herndon, and I. Gutman, *Tetrahedron Lett.*, 755 (1975).
- (21) E. Clar and W. Schmidt, *Tetrahedron*, **35**, 2673 (1979).
- (22) The p-band energies correlate¹¹ linearly with IP_1 (slope 1.402), the α - and β -band energies with IP (slopes 0.886 and 1.516, respectively).
- (23) E. Clar and W. Schmidt, to be published.
- (24) E. Clar, W. Schmidt, and T. Zauner, to be published.